Showcasing research from Professor Pimchai Chaiyen's laboratory, School of Biomolecular Science and Engineering, Vidyasirimedhi Institute of Science and Technology (VISTEC), Rayong, Thailand.

Red-shifted D-luciferin analogues and their bioluminescence characteristics

Reactions of luciferases and luciferins found in various organisms can generate bioluminescence or cold light emission useful as analytical and visualization tools. Here, six new D-luciferin analogues were synthesized. All analogues produce light with longer wavelengths compared to native D-luciferin. Notably, 5'-methyl- and 5',7'-dimethyl-D-luciferin generate brighter, red-shifted, and longer-lasting signals across multiple luciferases. Both analogues showed high sensitivity in mammalian cell assays. These red-shifted D-luciferin analogues are valuable for improving luciferase applications in biomedical research because they would allow better light penetration through cells, blood and tissue of animal models.

Image reproduced by permission of Pimchai Chaiyen from
RSC Chem. Biol., 2026, **7**, 67.

ROYAL SOCIETY
OF **CHEMISTRY**

rsc.li/rsc-chembio

ROYAL SOCIETY OF CHEMISTRY

Check for updates

Red-shifted D-luciferin analogues and their bioluminescence characteristics

Pratchaya Watthaisong,[a] Chadaporn Kantiwiriyawanitch,[a] Watcharapa Jitkaroon,[a] Aisaraphon Phintha, [ID][a] Ittiphat Klayparn,[a] Narin Lawan, [ID][b] Philaiwarong Kamutira,[a] Daisuke Sasaki,[c] Surawit Visitsatthawong,[a] Somchart Maenpuen,[d] Ruchanok Tinikul,[e] Jeerus Sucharitakul,[f] Ryo Nishihara, [ID][g] Kazuki Niwa, [ID][h] Yoshihiro Nakajima, [ID][c] Yoshihiro Ohmiya[ai] and Pimchai Chaiyen [ID] *[a]

D-Luciferin (D-LH$_2$) is the most used substrate for beetle luciferases in various bioluminescence applications. Here, we successfully synthesized six D-LH$_2$ analogues including 5′,7′-dimethoxy-D-LH$_2$ and 7′-methylnaphthol-D-LH$_2$ as novel compounds. We also developed a continuous one-pot green synthesis method to improve yields of luciferins from condensation of quinone and D-Cys (63-fold greater than the previous report). The novel D-LH$_2$ analogues were tested with five luciferases (Fluc, SLR, Eluc, Pmluc-WT, and Pmluc-N230S), and all the compounds emitted bioluminescence at wavelengths longer than that of D-LH$_2$ (>80 nm). The reaction of SLR with 5′,7′-dimethoxy-D-LH$_2$ gave the longest red-shifted bioluminescence at 663 nm. Remarkably, the reactions of 5′-methyl-D-LH$_2$ emit longer wavelengths and brighter light than those of D-LH$_2$ in all tested luciferases, except for Eluc. Interestingly, the novel red-shifted 5′,7′-dimethyl-D-LH$_2$ also provided prolonged bioluminescence with a rate of light decay slower than that of D-LH$_2$. We further demonstrated applications of 5′-methyl-D-LH$_2$ and 5′,7′-dimethyl-D-LH$_2$ in mammalian cell lines expressing Fluc, SLR, and Pmluc-N230S. 5′-Methyl-D-LH$_2$ provided about 11.2-fold greater sensitivity to detect Fluc in the HEK293T crude lysate than D-LH$_2$, achieving the detection with a lower number of cell lines. The red-shifted 5′,7′-dimethyl-D-LH$_2$ also exhibits high sensitivity when using a red light filter to monitor live cell bioluminescence. These D-LH$_2$ analogues, 5′-methyl-D-LH$_2$ and 5′,7′-dimethyl-D-LH$_2$, are promising substrates for future cell-based assays and real-time monitoring applications.

[a] *Biomolecular Science and Engineering (BSE), Vidyasirimedhi Institute of Science and Technology (VISTEC), Wangchan Valley, Rayong, 21210, Thailand. E-mail: pimchai.chaiyen@vistec.ac.th*

[b] *Department of Chemistry, Faculty of Science, Chiang Mai University, Chiang Mai, Thailand*

[c] *Health and Medical Research Institute, National Institute of Advanced Industrial Science and Technology (AIST), Takamatsu, Kagawa 761-9035, Japan*

[d] *Department of Biochemistry, Faculty of Science, Burapha University, Bangsaen, Chon Buri District, Chon Buri 20131, Thailand*

[e] *Department of Biochemistry, Faculty of Science, Mahidol University, Ratchathewi, Bangkok 10400, Thailand*

[f] *Department of Biochemistry, Faculty of Science, Chulalongkorn University, Pathum Wan, Bangkok 10330, Thailand*

[g] *Health and Medical Research Institute, National Institute of Advanced Industrial Science and Technology (AIST), Tsukuba, Ibaraki 305-8566, Japan*

[h] *National Metrology Institute of Japan, National Institute of Advanced Industrial Science and Technology (AIST), Tsukuba, Ibaraki 305-8563, Japan*

[i] *Department of Biomedical Engineering, Osaka Institute of Technology (OIT), Osaka, Japan*

Introduction

Reactions of luciferases and luciferins found in various organisms can generate cold light emission or bioluminescence (BL). These reactions are efficient analytical and visualization tools which have been applied in various detection technologies.[1] It has been estimated that nearly 30% of high-throughput screening (HTP) reactions used in academia and industry involve luciferase reactions.[2] Beetle luciferases, especially firefly luciferases (Fluc), are among the most widely used BL systems in biochemical and cell-based assays because of their catalytic oxidation of the D-luciferin (D-LH$_2$) substrate to oxyluciferin generates green-yellow light ($\sim$560 nm) with a high quantum yield (41%).[2,3] Although the Fluc reaction is useful for a variety of assays, its application for *in vivo* imaging is limited because BL signals generated by the natural D-LH$_2$ emits green-yellow light which does not penetrate well into animal cells or tissues. The current use of D-LH$_2$ in animal experiments requires the usage of high doses, thus resulting in high experimental cost.[4,5] D-LH$_2$ analogues with red-shift and steady

© 2026 The Author(s). Published by the Royal Society of Chemistry

RSC Chem. Biol., 2026, **7**, 67–80 | 67

BL are thus valuable for improving Fluc applications because this would allow better light penetration through the cells, blood and tissues of animal models.[6]

Numerous D-LH$_2$ analogues particularly in the forms of 6′-aminoluciferin (6′-NH$_2$LH$_2$) and cyclic alkylaminoluciferin (CycLuc1) emit red-shifted BL.[7] The longest wavelengths could be achieved with AkaLumine–HCl and its derivatives including seMpai (up to 675 nm)[8] and infraluciferin (iLH$_2$, >700 nm).[7,8] However, their applications are still challenging because the natural Fluc (the most widely used luciferase for general applications) does not utilize these D-LH$_2$ analogues well. Several enzyme engineering campaigns were carried out to evolve luciferases suitable for using these compounds and increase the BL intensity.[8–10] Although the engineered luciferase, namely Akaluc, could use AkaLumine–HCl as a substrate and exhibit brighter BL than the native Fluc,[7,11] the overall signals are still low.

This is due to the low quantum yield of AkaLumine–HCl with Fluc (4.0 ± 0.5%), which is significantly lower than that of natural D-LH$_2$.[12] Therefore, new red-shifted D-LH$_2$ analogues which can be used as dropped-in substrates for the native beetle luciferases would provide alternative choices for biomedical researchers to directly use the widely available beetle luciferase systems to generate red-shifted BL for cell-based screening applications.

Currently, the synthesis of D-LH$_2$ and most of its analogues at a scale of >50 mg can only be performed through chemical methods which typically require multi-step organic synthesis and purification (∼4 steps). The chemical reactions need to be carried out at 120–190 °C using hazardous chemicals such as acetic anhydride (Ac$_2$O), pyridine, sulfolane, and dimethylformamide (DMF)[13–15] by highly skilled chemist experts. We previously reported the chemo-enzymatic synthesis of novel D-LH$_2$ analogues with methyl substituent groups at the benzothiazole ring of D-LH$_2$ which gave a red shift in emission up to 620 nm with good BL intensity and light stability. These compounds can be used directly as substrates for the native Fluc and have been demonstrated as environmental monitoring tools without Fluc engineering.[16] Our methodology was based on the condensation of benzoquinone (BQ) and D-cysteine (D-Cys) to form the D-LH$_2$ using the HadA enzyme (HELP, HadA Enzyme for Luciferin Preparation);[17,18] the process was optimized to obtain a high yield of D-LH$_2$ analogues of about ∼51% with a 7.1 mg yield at the 0.5 L scale.[16] Although the HELP process is green, its scale up is still limited when compared to other conventional chemical synthesis methods because it utilizes the HadA and associated enzymes.

In this work, we developed a cost-effective one-pot green synthesis procedure for methyl-, methoxy-, and naphthol-D-LH$_2$ analogues using the condensation reaction of BQ derivatives and D-Cys without adding the HadA and auxiliary enzymes. The process was optimized to improve the product yield for the bulk scale and easy preparation of D-LH$_2$ analogues while providing compatibility with green chemistry principles[19] (Fig. 1a). We have used the method to prepare six methyl-, methoxy and naphthol-substituted D-LH$_2$ analogues including natural

D-LH$_2$ (2a), 5′-methyl-D-LH$_2$ (5′-MeLH$_2$, 2b),[16] 5′,7′-dimethyl-D-LH$_2$ (5′,7′-DiMeLH$_2$, 2c),[20] and 4′,7′-dimethyl-D-LH$_2$ (4′,7′-DiMeLH$_2$, 2e)[21] with two novel luciferins: 5′,7′-dimethoxy-D-luciferin (5′,7′-DiOMeLH$_2$, 2d) and 7′-methylnaphthol-D-luciferin (7′-MeNpLH$_2$, 2f). With an appropriate substrate ratio and continuous addition of substrates under anaerobic conditions, the developed one-pot green synthesis approach can preserve the stability of BQ derivatives and D-Cys, preventing substrate deterioration, reducing byproduct formation and increasing D-luciferin analogue yield (by 63-fold relative to that of the previously reported chemical condensation method,[17] Fig. 1b and 1c). The synthesized D-LH$_2$ analogues (2a–2f) were tested with five known beetle luciferases including *Photinus pyralis* luciferase (Fluc), *Phrixothrix hirtus* red-emitting luciferase (SLR), *Pyrearinus termitilluminans* emerald luciferase (Eluc), *Pyrocoelia miyako* luciferase wild-type (Pmluc-WT), and the *Pyrocoelia miyako* luciferase variant (Pmluc-N230S) commonly used in BL applications[22–26] (Fig. 1d). Their biochemical, steady-state kinetics and BL properties of these enzymatic reactions were characterized (Fig. 1e and f). The novel methyl- and methoxy-D-LH$_2$ analogues demonstrated their better red-shifted BL (>600 nm), increased brightness, and slow decay rate of BL emission compared to the reaction of natural D-LH$_2$ (2a). 5′-Methyl-D-LH$_2$ and 5′,7′-dimethyl-D-LH$_2$ which showed promising BL characteristics in enzymatic reactions were further explored for their *in vivo* BL properties in mammalian cell lines expressing Fluc, SLR, and Pmluc-N230S. These newly discovered unique properties of methyl-D-LH$_2$ compounds provide the unique BL characteristics advantageous for future cell-based assays and real-time monitoring applications.

Results and discussion

Synthesis of D-LH$_2$ analogues and their yield optimizations

We investigated the condensation of various BQ (1a) derivatives and D-Cys to synthesize D-LH$_2$ analogues with more red-shifted light emission (Fig. 2a). High-resolution quadrupole time of flight mass spectrometry (QTOF-MS) was used for identifying potential products. The results (Table S1) revealed that the BQ derivatives (1a–1f) can serve as electrophilic substrates (Fig. 2b) for the D-Cys condensation reaction, producing the D-LH$_2$ analogues (2a–2f) shown in Fig. 2c. Structures of the novel D-LH$_2$ analogues were elucidated by LC/QTOF-MS and NMR (Tables S1–S3) as 5′,7′-DiOMeLH$_2$ (2d) and 7′-MeNpLH$_2$ (2f), as shown in Fig. 2c. These compounds were not previously found in nature nor reported.

Previously, the yield of D-LH$_2$ (2a) obtained using BQ (1a) and D-Cys condensation alone was poor (0.3%).[17] We hypothesized that this was due to the instability of 1a. We thus screened for buffers and reaction conditions which might be suitable for providing better yields. Results in Fig. S1 indicate that the organic buffer, 100 mM HEPES, gave the highest D-LH$_2$ yield compared to other systems. We further explored co-solvent systems to stabilize 1a and enhance the yield of D-LH$_2$ synthesis of 2a. We found that the addition of 20% (v/v) methanol
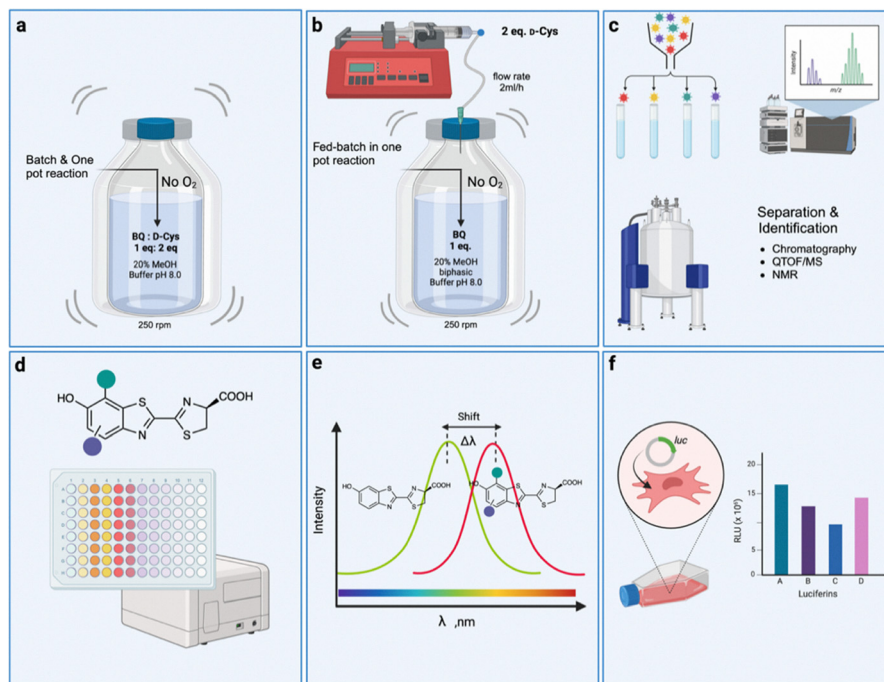
Fig. 1 Graphical representation of the overall workflow. (a) Batch and one-pot reaction for D-LH$_2$ synthesis. (b) Fed-batch synthesis of D-LH$_2$ analogues in one-pot reaction. (c) D-LH$_2$ analogues were isolated and characterized and their structures were elucidated by ^{1}H and ^{13}C NMR and high-resolution mass spectrometry. (d) BL reactions of new D-LH$_2$ analogues with five types of beetle luciferases. (e) BL characteristics of novel D-LH$_2$ analogues. (f) Demonstration of applications for new D-LH$_2$ analogues in mammalian cell line assays and real-time bioluminescence monitoring of live cells.

increased the yield of **2a** formation by about 2.8-fold compared to the system without any solvent addition (Fig. S2). We further identified a bottleneck of **1a** and D-Cys condensation by varying the percentage of oxygen in the reaction. The reaction buffers were prepared by equilibration with various concentrations of O$_2$ (<0.0005%, 10%, and 20%) and used in the reactions to monitor the product **2a** formed. The results in Fig. 3a reveal that low concentrations of O$_2$ tend to improve the yield of **2a** formation, possibly by preventing the decay of **1a** to another form. With <0.0005% O$_2$ (anaerobic condition), the reaction gave the highest yield of **2a** formation which was greater than that of the 20% O$_2$ (air-saturation) condition by about 1.8-fold with a D-LH$_2$ formation rate of 3.26 μM h^{-1} (Fig. S5 and Table S4).

After finding that the instability of the **1a** derivatives and D-Cys substrates is a limiting factor for the generation of D-LH$_2$ analogues, we designed a flow chemistry strategy by continuously mixing one substrate with another under various conditions. Fig. 3b illustrates the reactions to generate **2a** in batch and continuous feeding (fed-batch) systems. Due to the O$_2$ vulnerability of the substrates, only low percentages of **2a** formation (up to 18%) could be obtained from the batch reactions within 24 h. For the continuous feeding of **1a** into the anaerobic buffer containing 2 (orange) and 4 (old rose) equivalents (eq.) of D-Cys, the yield of **2a** formation was about twice that of the batch reactions (Fig. 3b, orange bar at 24 h). Remarkably, when 2 equivalents (eq.) of D-Cys were pumped into 1 eq. of **1a** under anaerobic conditions, the highest yield of **2a** formation (about 86 μM) could be obtained (Fig. 3b, pink bar

at 24 h). This yield was 16.4-fold greater than that of the batch reaction after 12 h (Fig. 3b). Therefore, by pumping 2 eq. of D-Cys into a 1 eq. solution of **1a** under anaerobic reactions (Fig. 3c), the stability of the substrates could be greatly enhanced and the reaction could be finished after 8 h (Fig. 3d).

To synthesize D-LH$_2$ analogues at a semi-large scale, our method described above and the recently published protocol[27] of using BQ, L-Cys methyl ester and D-Cys to synthesize D-LH$_2$ were tested. We found that **2a** and **2c** compounds could be prepared with 50 and 66% yield, respectively, when using the BQ derivatives (**1a** and **1c**) and the L-Cys methyl ester and D-Cys condensation protocol. However, this protocol could not be used to prepare other D-LH$_2$ analogues (compounds **2b** and **2d**) because it gave a mixture of products (non-specific reactions in the case of **2b** synthesis) and the electron-donating group of **1d** affected the cyclization of the benzothiazole ring (in the case of **2d** synthesis). These compounds could only be prepared using a fed-batch reaction shown in Fig. 3 and described above. The fed-batch protocol developed in this work is thus useful for synthesizing D-LH$_2$ analogues without utilizing harmful catalysts or toxic chemicals. The reaction also requires less usage of organic solvent and thus is compatible with green chemistry principles. These findings set an important foundation for future large-scale production of the compounds.

NMR, mass spectra, absorption, and fluorescence characteristics of D-LH$_2$ analogues

The method described in the previous section was used to synthesize D-LH$_2$ analogues (**2a–2f**) from the BQ derivative

© 2026 The Author(s). Published by the Royal Society of Chemistry

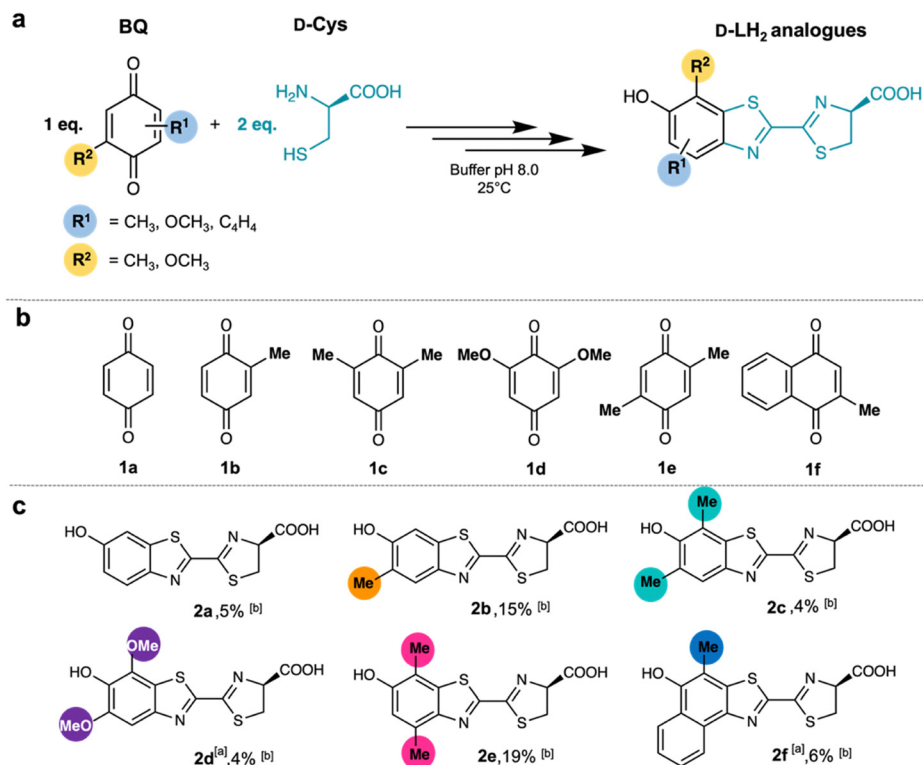*RSC Chem. Biol.*, 2026, **7**, 67–80 | **69**

Fig. 2 Synthesis of D-LH$_2$ and its analogues by condensation of D-Cys and BQ derivatives. (a) D-LH$_2$ and its derivatives could be obtained under batch conditions. (b) BQ derivatives (1a−1f) serve as substrates for synthesizing D-LH$_2$ analogues. (c) The D-LH$_2$ analogues (2a−2f) obtained from condensation of D-Cys and BQ derivatives (1a−1f). [a] Novel D-LH$_2$ analogues are 5′,7′-DiOMeLH$_2$ (2d) and 7′-MeNpLH$_2$ (2f). [b] Isolated yields of D-LH$_2$ analogues after purification.
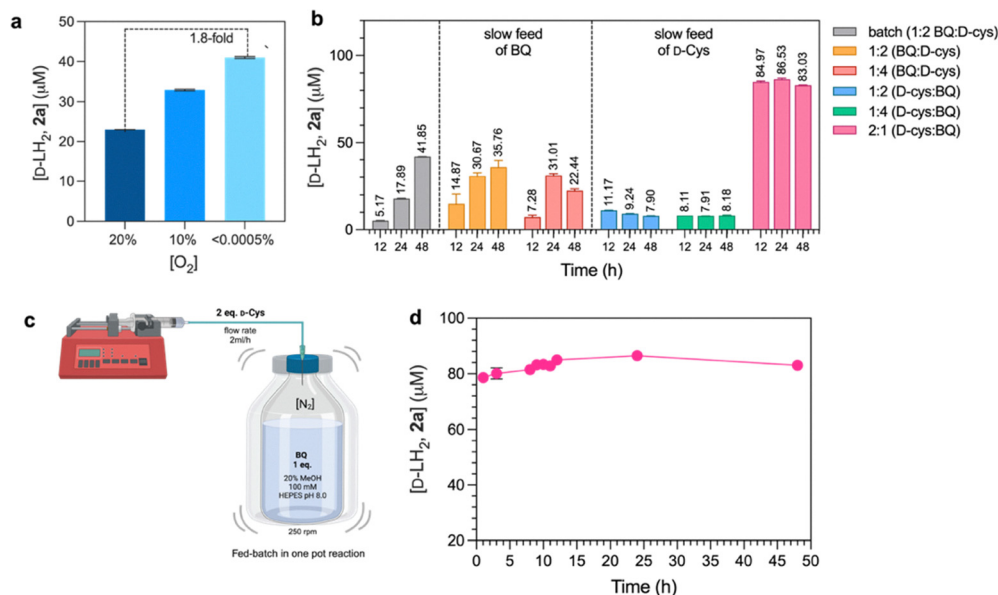

Fig. 3 Optimization of 2a production yield. (a) Effects of O$_2$ concentrations on 2a formation. (b) Synthesis of 2a by pumping a solution of one substrate into another substrate solution with different ratios under anaerobic conditions. (c) The synthesis of 2a could be set up by continuously feeding 2 eq. of D-Cys (2 mL h^{-1}) into 1 eq. of 1a under anaerobic conditions. (d) Kinetics of continuous formation of 2a by feeding 2 eq. of D-Cys (2 mL h^{-1}) into 1 eq. of 1a under anaerobic conditions.

substrates (1a−1f, Fig. 1b). The products were isolated (purity up to 97%), and their structures were characterized using QTOF-MS and NMR spectroscopy (Fig. 1c and Fig. S3 and S4 and Tables S3 and S4). The observed m/z with low mass error

values of D-LH$_2$ analogues (**2a**–**2f**) from the QTOF-MS data (Table S1) confirmed that the BQ derivatives (**1a**–**1f**) can react with D-Cys to yield the products in one-pot synthesis. The structures of **2a**–**2f** were then elucidated using ^{1}H NMR (Fig. S3 and Table S2) and ^{13}C NMR (Fig. S4 and Table S3) to identify the molecular structures of the D-LH$_2$ analogues. The NMR results indicate that the benzothiazole rings of the D-LH2 analogues were substituted with methyl and methoxy groups at 4′, 5′, and 7′-positions (Fig. 2c) and demonstrated that we could obtain novel compounds including 5′,7′-DiOMeLH$_2$ (**2d**) and 7′-MeNpLH$_2$ (**2f**). All of the D-LH$_2$ analogues (**2b**–**2f**) were further investigated for their absorption and fluorescence characteristics in comparison with the native D-LH$_2$ (**2a**) as described below.

Absorption and fluorescence characteristics of D-LH$_2$ analogues (**2a**–**2f**) in 100 mM HEPES pH 8.0 at 25 °C were recorded. The natural D-LH$_2$ (**2a**) displayed a maximum adsorption peak (λ_{max}) at 327 nm, while **2b** which has a methyl group addition at the 5′-position of the benzothiazole moiety also gave a similar λ_{max} at 323 nm (Table S6). However, for **2c** and **2e** which have two methyl substitutions at the benzothiazole skeleton, their absorption spectra shifted to longer wavelengths of λ_{max} at 334 and 330 nm, respectively (Table S5). The addition of dimethoxy (**2d**) and naphthol groups (**2f**) resulted in longer wavelength shifts (λ_{max} at 412 and 437 nm, respectively) (Table S5). Similarly, the fluorescence properties of natural D-LH$_2$ (**2a**) and methyl-D-LH$_2$ analogues (**2b**, **2c**, and **2e**) showed similar fluorescence emission spectra with peaks around 523–560 nm. For **2d** and **2f**, their emission spectra showed a greater bathochromic shift with the peaks around 620 and 580 nm, respectively (Table S5). These absorption and fluorescence characteristics of the D-LH$_2$ analogues (**2a**–**2f**) provide a means by which BL can be red shifted (shown later). It should be noted that their uniqueness in fluorescence is also valuable for future use in florescence-based sensor applications.[28,29]

Bioluminescence characteristics of D-LH$_2$ analogues

The purified D-LH$_2$ analogues (**2a**–**2f**) were investigated for their BL characteristics using known luciferases, *i.e.*, Fluc, SLR, Eluc, Pmluc-WT, and Pmluc-N230S. Results in Fig. 4a showed that **2b**–**2f** could serve as substrates for various luciferases (except **2f**, which could not serve as a substrate for Pmluc-WT and Pmluc-N230S) and generate light emission with longer wavelengths (red-shifted) compared to the natural D-LH$_2$ (**2a**). Interestingly, the pairing of novel D-LH$_2$ analogues (**2d** and **2f**) with SRL and Fluc gave red light emissions at longer than 630 nm which could be recorded by a digital single-lens reflex (DSLR) camera (Fig. 4b–e). We found that a methyl substituent in the benzothiazole ring of D-LH$_2$ could also modulate absorption, fluorescence and BL characteristics of luciferases (Table S5). Particularly, the BL emission was altered from yellow-green (∼560 nm) of the natural D-LH$_2$ (**2a**) to be in the red-shifted region (>600 nm).

We also compared the photon emission of methyl-substituted D-LH$_2$ analogues **2b** and **2c** to that of the natural compound (**2a**) using an integrating sphere-based multichannel spectrometer

with a charge-coupled device (CCD) detector (details are given in SI, Section S1.5). The photon/pixel emission spectra of the luciferase reaction showed that red-shifted methyl-substituted D-LH$_2$ analogues (**2b** and **2c**) provided greater photon emission than that of the natural compound (**2a**). Interestingly, **2b** showed greater photon emission than those of **2a** in Fluc, SLR, and Pmluc-N230S reactions (Fig. 4f–i). The spectra of **2b** and **2c** also showed the emission wavelengths longer than 600 nm. BL properties of D-LH$_2$ analogues (**2a**–**2c**) correlate well with their quantum yields in the reactions of Fluc, SLR, and Pmluc-N230S measured later.

Importantly, the D-LH$_2$ analogues (**2b**–**2f**) in this study allowed the reactions of Fluc and other luciferases to gain a maximum BL emission band shift ($\Delta^{BL}\lambda$) of >40 nm and up to 88 nm compared to **2a** (Fig. 4j). The largest BL wavelength shift in this study could be obtained from the **2d**-SLR orthogonal pair that emitted a maximum light peak at 663 nm and a broad BL spectrum beyond 750 nm, which could be beneficial for bio-imaging and real-time deep tissue *in vivo* monitoring applications in the future.

Kinetics and thermodynamic properties of new D-LH$_2$ analogues with different luciferases

To investigate the substrate specificity and the influence of substituents of D-LH$_2$ analogues on BL characteristics, steady-state kinetics of luciferase (Fluc, SLR, Eluc, Pmluc-WT, and Pmluc-N230S) reactions using various D-LH$_2$ analogues (**2b**–**2f**) as substrates were carried out at 25 °C and pH 8.0 to measure their kinetic constant, K_m and k_{cat}, values compared to those of the natural D-LH$_2$ (**2a**). The results in Table S6 show that, for all luciferases studied, the K_m values of **2b** were comparable to those of **2a**, suggesting that a methyl group substituent at the 5′-position of luciferin′s benzothiazole ring (**2b**) does not interfere with the ability of the enzyme to interact and react with a substrate. It should be noted that while the natural D-LH$_2$ mostly exhibits strong substrate inhibition with a range of > 1–10 μM against various luciferases, D-LH$_2$ analogues (**2b**–**2f**) showed lower severity of substrate inhibition (Table S6). For the compounds with methoxy substituents at 5′ and 7′-positions or methyl substituents at the 4′ and 7′-positions, such as **2d**, **2e** and **2f**, their K_m values were mostly greater than those of **2a**, implying that these substituents may disrupt the interactions of these luciferins to serve as substrates for luciferases.

The k_{cat} values of the BL reactions indicate that the reactions of **2b** with various luciferases, Fluc, SLR, Pmluc-WT, and Pmluc-N230S, yielded k_{cat} values greater than those of the native substrate (**2a**). In particular, the reaction with Pmluc-N230S resulted in a 5.2-fold increase in the k_{cat} value. However, the stability of the light emission ($t_{1/2}$) of **2b** is very similar to that of **2a** in Fluc and Pmluc-WT, and light emission by SLR and Pmluc-N230S could be prolonged longer than those of other systems by about 1.5 and 1.7-fold, respectively (Fig. 5b). This result suggests that **2b** with a methyl substituent at the 5′-position of the benzothiazole skeleton does not display any adverse effects on the activities of luciferases or their BL properties. The reactions of **2c** exhibited k_{cat} values of
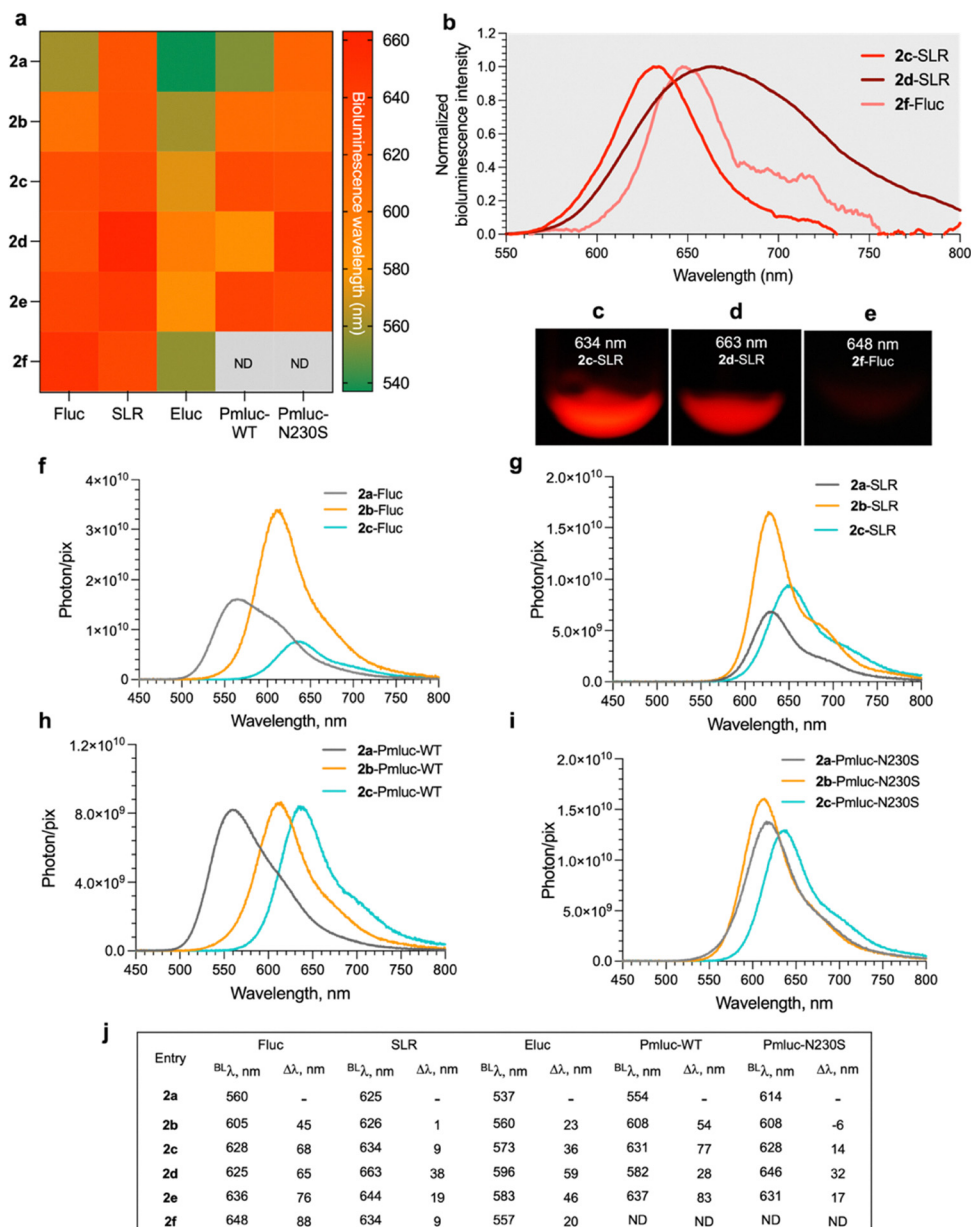
© 2026 The Author(s). Published by the Royal Society of Chemistry

RSC Chem. Biol., 2026, **7**, 67–80 | 71

Fig. 4 BL characteristics of D-LH$_2$ analogues (**2a–2f**) reacted with various luciferases. Reactions of various luciferases with D-LH$_2$ analogues (**2b–2f**) were carried out at 25 °C in 100 mM HEPES buffer at pH 8.0 and compared to those of natural D-LH$_2$ (**2a**). (a) Heat maps describing BL emission of D-LH$_2$ analogues (**2a–2f**) generated from their reactions with Fluc, SLR, Eluc, Pmluc-WT, and Pmluc-N230S luciferases. (b) BL emission spectra of novel D-LH$_2$ analogues (**2d** and **2f**) obtained from their reactions with their orthogonal luciferases. (c–e) BL signals obtained from the reactions of novel D-LH$_2$ analogues (**2d** and **2f**) and their orthogonal luciferases were recorded by a DSLR camera. (f–i) The BL emission spectra of the luciferase (5 μM)–luciferin (2 μM) reactions were measured using the integrating sphere-based multichannel spectrometer. (j) The difference in emission wavelengths of D-LH$_2$ analogues (**2b–2f**) compared to those of the natural D-LH$_2$. ND denotes the non-detectable signals.

approximately half that of **2a** (except in the reaction of SLR, in which **2c** gave a slightly higher k_{cat} than **2a** by approximately 1.3-fold). **2d–2f** provided very low bioluminescence intensity (BLI) in all luciferases tested (Fig. 5a and Table S7). The results indicate that **2d–2f** showed larger K_m and lower BLI values than the native substrate (**2a**) in most of the enzyme reactions investigated. The data indicate that reactions of **2d–2f** were not suitable with currently available luciferases and would require future work to engineer luciferases to obtain the best

orthogonal pair of luciferase-D-LH$_2$ analogues with high BLI. We noted that Eluc prefers to use **2a** as a substrate rather than other analogues (Fig. 5a and Table S6) based on the k_{cat} and K_m values, but other enzymes such as Fluc, SLR, Pmluc-WT, and Pmluc-N230S could use **2b** as an alternative substrate well. We also measured the stability of light emissions of the D-LH$_2$ analogues (**2a–2c**). The results in Fig. 5b clearly indicate that **2c** gave longer BL half-lives ($t_{1/2}$) than the natural D-LH$_2$ when using Fluc and Pmluc-N230S, by about 1.7- and 5.6-fold,
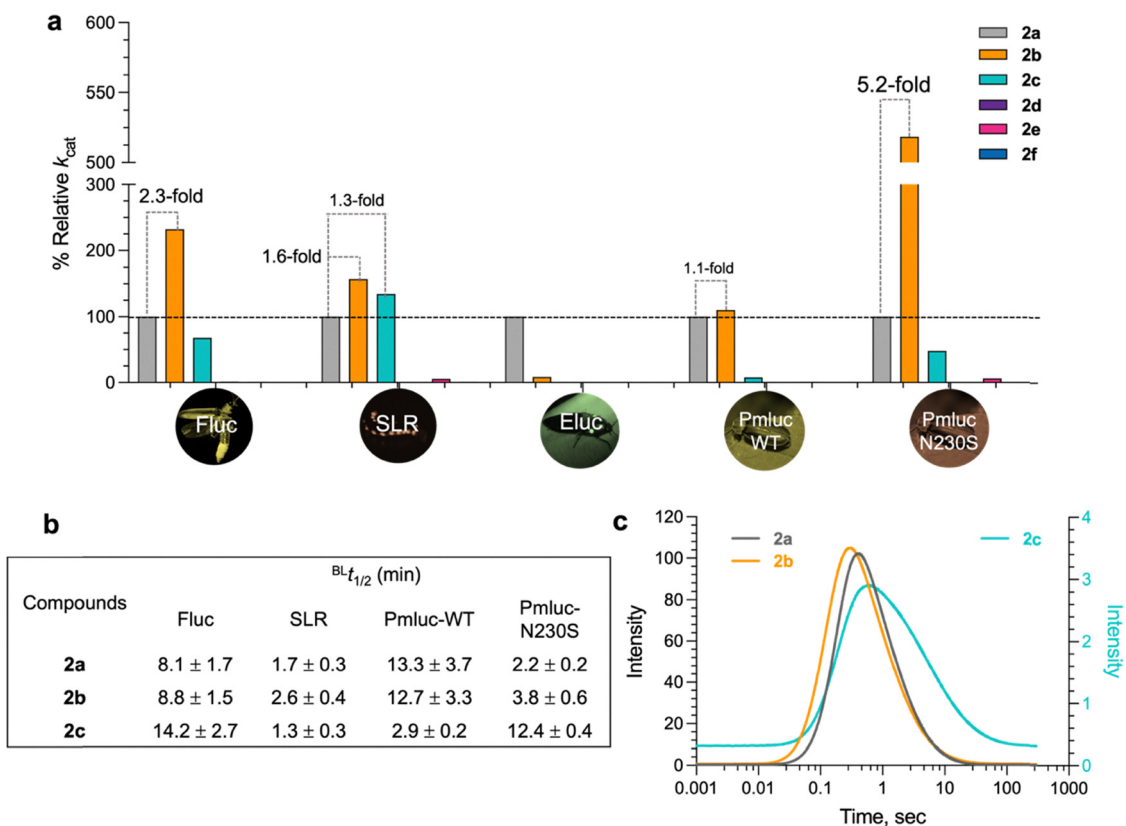
Fig. 5 BL characteristics of D-LH$_2$ analogues and luciferases. (a) The relative k_{cat}, which represents the BL intensity (BLI) of each D-LH$_2$ analogue (**2a–2f**) when it reacts with luciferases compared to those of **2a** reactions. (b) The half-time ($t_{1/2}$) values of BL emission of D-LH$_2$ analogues (**2a–2c**) which react well with Fluc, SLR, Pmluc-WT, and Pmluc-N230S luciferases. (c) Kinetics of light formation and light decay of Fluc reactions with D-LH$_2$ analogues (**2a–2c**) monitored by stopped-flow luminometry.

respectively, as compared to those of **2a**. Without the addition of coenzyme A (CoA), the ability of **2c** in prolonging BL in Fluc and Pmluc-N230S should be useful for future live-cell imaging applications. Thus, the current best substrate analogues of luciferases such as Fluc, SLR, Pmluc-WT, and Pmluc-N230S are **2b** and **2c** which are also promising substrates for red-shifted BL and steady light emission in the reaction of SLR. Although **2d** and **2f** are novel compounds with potentially useful long wavelength emission, their usage with native luciferases is not very efficient due to their low BL signals. This is due to non-compatibility of these compounds with native enzymes. Engineering campaign of beetle luciferases is required for improving their BL signals in the future.

To comprehensively characterize the bioluminescence properties of the D-LH$_2$ analogues (**2a–2d**), we measured their bioluminescence quantum yields from their reactions with Fluc, SLR, and Pmluc-N230S. The reactions were performed using the conditions obtained from steady-state kinetics studies (Fig. 5a and Table S6). Results shown in Table 1 and Table S8 indicate that the reaction of Fluc with **2b** gave the greatest quantum yield (0.52) and the value was higher than those of the natural D-LH$_2$ and other D-LH$_2$ analogues. The data clearly support potential applications of Compound **2b**. For the reactions with SLR and Pmluc-N230S, compounds **2a–2c** showed the same range of quantum yields. However, the

Table 1 Quantum yields of luciferases and D-LH$_2$ analogues

Luciferins	Quantum yield with different luciferases		
	Fluc	SLR	Pmluc-N230S
2a	0.44 ± 0.04	0.160 ± 0.005	0.160 ± 0.018
2b	0.52 ± 0.01	0.190 ± 0.005	0.170 ± 0.034
2c	0.200 ± 0.007	0.160 ± 0.003	0.150 ± 0.014
2d	ND^a	ND^a	ND^a

^{a} ND denotes "not determined" because **2d** gave low bioluminescence signals.

quantum yield of Compound **2d** with all luciferases could not be measured due to low bioluminescence signals. Altogether, the results of quantum yield measurements indicate that the Fluc-**2b** pair gives the greatest value of BL signals.

Furthermore, the equilibrium binding constant (K_d) values of D-LH$_2$ analogues (**2b–2d**) with Fluc were measured using isothermal titration calorimetry (ITC) and compared with the values of natural D-LH$_2$ (**2a**). The results in Table 2, Table S9 and Fig. S7 reveal that the K_d value of **2b** was about half that of **2a**, indicating that **2b** has a greater binding affinity to Fluc than **2a**. The data suggest that the 5′-methyl substituent in **2b** does not interfere with the binding interactions between the substrate and the Fluc pocket site but rather promotes a tighter binding. For other D-LH$_2$ analogues, the results indicate that

Table 2 Thermodynamics of ligand binding and kinetics constants for light formation and decay of the reactions of D-LH$_2$ analogues (**2a–2c**) with Fluc

	Dissociation constant (K_d, μM)		Observed rate constant (k_{obs})		
				Light decay (s^{-1})	
Compound	Fluc: Luciferin[a]	Fluc-ApCPP: Luciferin[b]	Light formation (s^{-1})	Faster phase	Slower phase
2a	21.1 ± 7.4	4.2 ± 0.1	6.64 ± 0.05	1.57 ± 0.02	0.29 ± 0.00
2b	13.4 ± 2.5	4.00 ± 0.02	9.63 ± 0.04	1.55 ± 0.15	0.27 ± 0.00
2c	35.1 ± 3.1	25.3 ± 1.1	7.28 ± 0.02	0.27 ± 0.00	0.05 ± 0.00
2d	30.4 ± 8.2	—[c]	8.13 ± 0.08	0.50 ± 0.00	ND[d]
2e	NC[e]	864 ± 7	—[c]	—[c]	—[c]

[a] The K_d values were measured by titration between Fluc and luciferins. [b] The K_d values were measured by titration between Fluc-ApCPP complex and luciferins. To probe interactions between D-LH$_2$ analogues and the Fluc-ATP complex, we used the non-hydrolyzable ATP analogue (ApCPP, Adenosine-5'-[(α,β)-methyleno]triphosphate) instead of ATP. [c] —Denotes "not measured". [d] ND denotes "not determined" because **2d** kinetics gave only one decay phase. [e] NC denotes "not calculated" by ITC because **2e** gave a very high K_d value with Fluc.

modification of the luciferin benzothiazole ring at the 5'- and 7'-positions with methyl (**2c**) and methoxy groups (**2d**) yielded K_d values comparable to that of **2a**, indicating that these substituents also do not interfere with the binding behavior. To investigate whether the pre-binding of ATP can enhance the interactions of D-LH$_2$ analogues (**2b–2d**) with Fluc, we measured K_d values for binding of D-LH$_2$ analogues to the preformed complex of Fluc and adenosine-5'-[(α,β)-methyleno]triphosphate (ApCPP) (Table 2 and S9). ApCPP is an ATP analogue mimicking the adenylated-ATP intermediate structure which does not allow Fluc to proceed with catalysis. This Fluc-ApCPP complex thus allowed us to probe interactions between D-LH$_2$ analogues and the Fluc-ATP complex. Results in Table S9 indicate that all binding of D-LH$_2$ analogues exhibited lower K_d values in the Fluc-ApCPP complex, implying that the presence of ATP enhances stronger interactions of D-LH$_2$ analogues with Fluc.[30]

We also performed stopped-flow experiments to determine the observed rate constants (k_{obs}) of single turnover reactions of light formation and decay of the Fluc reactions with **2a–2c** (Fig. 5c and Table 2). The BL kinetics revealed three exponential phases (Fig. S6). The first phase was light formation, while the second and third phases were light decay with faster and slower rate constants, respectively. The kinetic analysis showed that all compounds displayed comparable k_{obs} values of light formation, suggesting that the substituents of D-LH$_2$ analogues synthesized in this work do not affect the light formation kinetics. Interestingly, the k_{obs} values of light decay in both faster and slower phases of the **2c** reaction were about 5–6-fold slower than those of **2a** and **2b**, indicating that the overall light emission yield in the reaction with **2c** would be much greater than those of **2a** and **2b**.

We then used molecular docking and molecular dynamics (MD) simulations to explain the binding and kinetic behaviors of the D-LH$_2$ analogues and luciferases as shown in Fig. S8–S19. The data revealed that all D-LH$_2$ analogues (**2b–2e**) can bind to the active site of Fluc (Fig. S8a–e). To further investigate the stability of the enzyme and D-LH$_2$ analogue complexes, MD simulations were performed across a range of temperatures (300–360 K). Results in Fig. S9–S18 showed that the structure of Fluc with **2a** and **2b** bound remained stable across all temperatures tested, particularly at the elevated temperature of 360 K

compared to that of Fluc with **2c** bound. These findings suggest that **2a** and **2b** exhibit stronger binding to Fluc compared to **2c**; these data correlate well with K_d values obtained from the ITC experiments (Table 2).

In order to explain the equilibrium binding constant (K_d) values of D-LH$_2$ analogues (**2b–2d**) with Fluc, the crystal structure of the luciferase enzyme (Fluc) from *Photinus pyralis* with adenylate analogue (DLSA) bound (PDB: 4G36) was analyzed. Residues within 6 Å of the 7'-position of the bound DLSA are shown in Fig. S19. The 7'-position of DLSA is surrounded by the helix (F247 and T251), the lower beta strand (L286), the middle beta strand (A313 and S314), the middle loop (G315 and G316), and two upper beta strands (Q338, G339, Y340 and A348, L350, I351) which are linked by the top loop (S347). The introduction of a methyl substituent at the 5'-position could interact with T251, leading to the lower K_d of **2b** compared to **2a**. In contrast, the introduction of a methyl substituent at the 7'-position could clash with the middle beta strand (A313 and S314) and the upper beta strand (Q338, G339, Y340) leading to the higher K_d of **2c** and **2d** compared to **2a**.

The overall data reported here indicate that **2b** and **2c** can be used well as dropped-in substrates for the currently available luciferases without requiring any enzyme engineering to provide red-shifted, high BL signals, and good light stability which could be useful for live-cell and animal BL applications in the future.

Demonstration of the use of D-LH$_2$ analogues in Mammalian cell assays

We tested the ability of the purified D-LH$_2$ analogues (**2a–2f**) to serve as substrates for Fluc expressed in mammalian cell lines including HepG2, HEK293T, HeLa, and RAW264.7. These cells are commonly used as hosts for monitoring the gene expression, cellular activities and molecular reactions of diseases.[8,31–34] BL signals generated by expression of Fluc in these cells have been used as tools to address various research topics in biomedical research. We transfected mammalian cells with the plasmid pGL4.13 expressing Fluc (details are given in SI, Section S1.6). Cells were collected after 24 h of growth for lysis, and the crude lysates were then assayed using the D-LH$_2$ analogue cocktail reagents (**2a–2f**). The results showed that **2b** provided light intensities similar to those of **2a** with the crude lysates of HepG2, HeLa, and RAW264.7 (Fig. 6a). Interestingly, **2b**
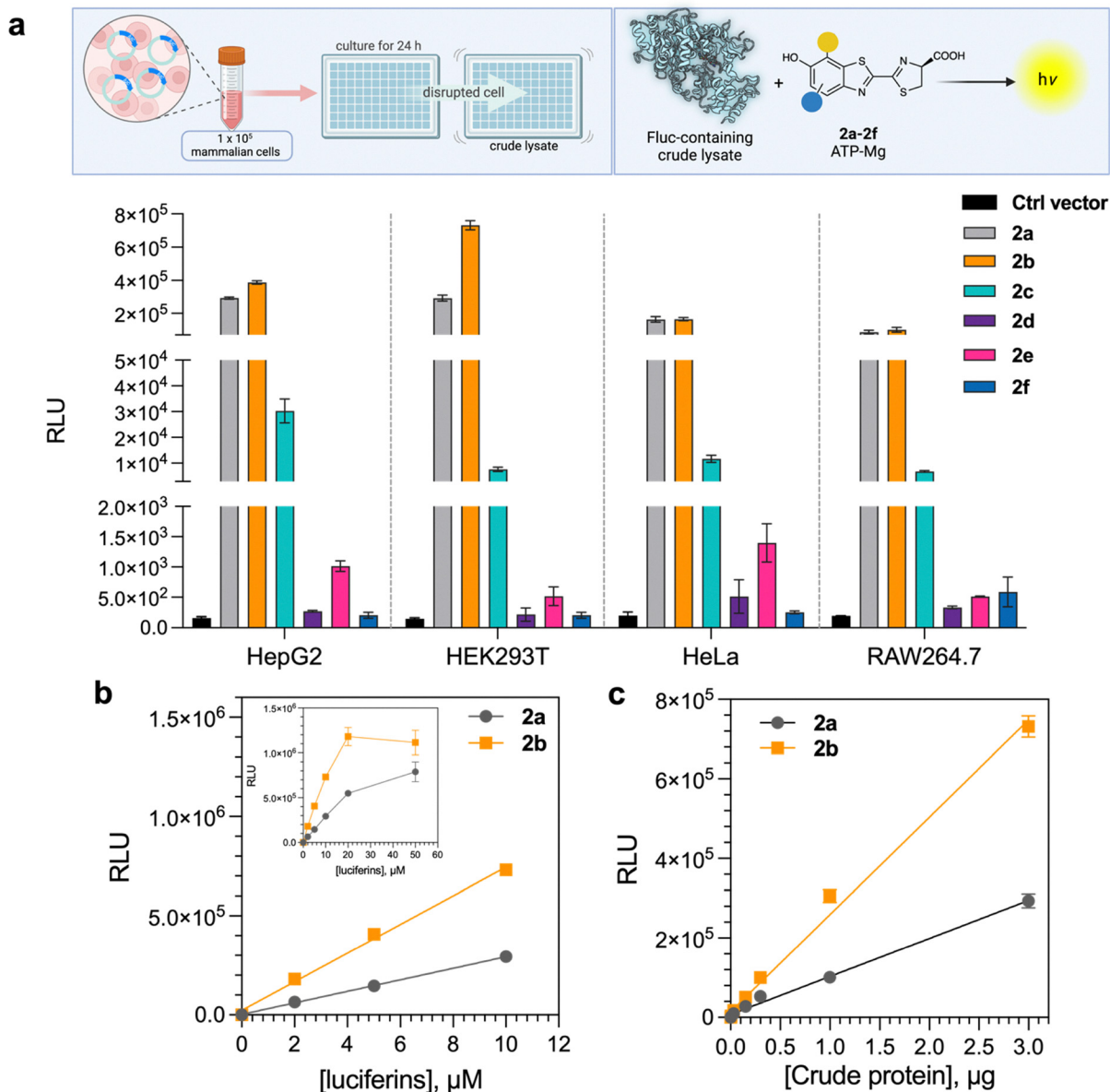
74 | *RSC Chem. Biol.*, 2026, **7**, 67–80

© 2026 The Author(s). Published by the Royal Society of Chemistry

Fig. 6   Applications of D-LH$_2$ analogues (**2a–2f**) in mammalian cell line BL assays. (a) The crude lysate of each cell line was tested with D-LH$_2$ analogues (**2a–2f**). (b) Comparison of light intensity from reactions of the Fluc-containing HEK293T crude lysate with 5′-MeLH$_2$ (**2b**) and natural D-LH$_2$ (**2a**) at various concentrations. (c) Dependence of light intensity on various concentrations of natural D-LH$_2$ (**2a**) and 5′-MeLH$_2$ (**2b**).

showed a higher light intensity in the HEK293T crude lysate than **2a**. In addition, **2c** exhibited good light intensity with HepG2, HEK293T, HeLa, and RAW264.7 cell lysates, whereas other analogues (**2d–2f**) gave poor light intensity (Fig. 6a). All results suggested that **2b** has good potential to be used as a substrate to generate red-shifted signals in BL applications because it can be used directly in commonly used cell-based assays with the wild-type Fluc.

We then further investigated the BL properties of **2b** by varying its concentration in the reaction with a fixed amount of HEK293T crude lysate and compared the light intensity with that produced by the native substrate **2a**. The results in Fig. 6b clearly demonstrated that **2b** gave greater light intensity than **2a** by about 2.5-fold. We then varied the concentrations of **2a** and **2b** with a fixed amount of HEK293T lysate and then varied the cell lysate amount with a fixed concentration of both compounds. The results as shown in Fig. 6b and c indicate that **2b** provided greater sensitivity than **2a** by about 2-fold.

The limit of detection (LOD) of expressed Fluc in crude cell lysates using **2a** and **2b** was identified to be 51.6 and 4.6 ng, respectively, indicating that **2b** can give a better sensitivity than the natural D-LH$_2$ (**2a**) by about 11.2-fold. Altogether, these results also confirmed that 5′-MeLH$_2$ (**2b**) can serve as a promising substrate for future cell-based assay applications.

Bioluminescence characteristics of D-LH$_2$ analogues in live cell applications

To demonstrate the use of D-LH$_2$ analogues (**2a–2c**) in live cells, we measured the BL spectra of **2a–2c** in the HepG2 cell line
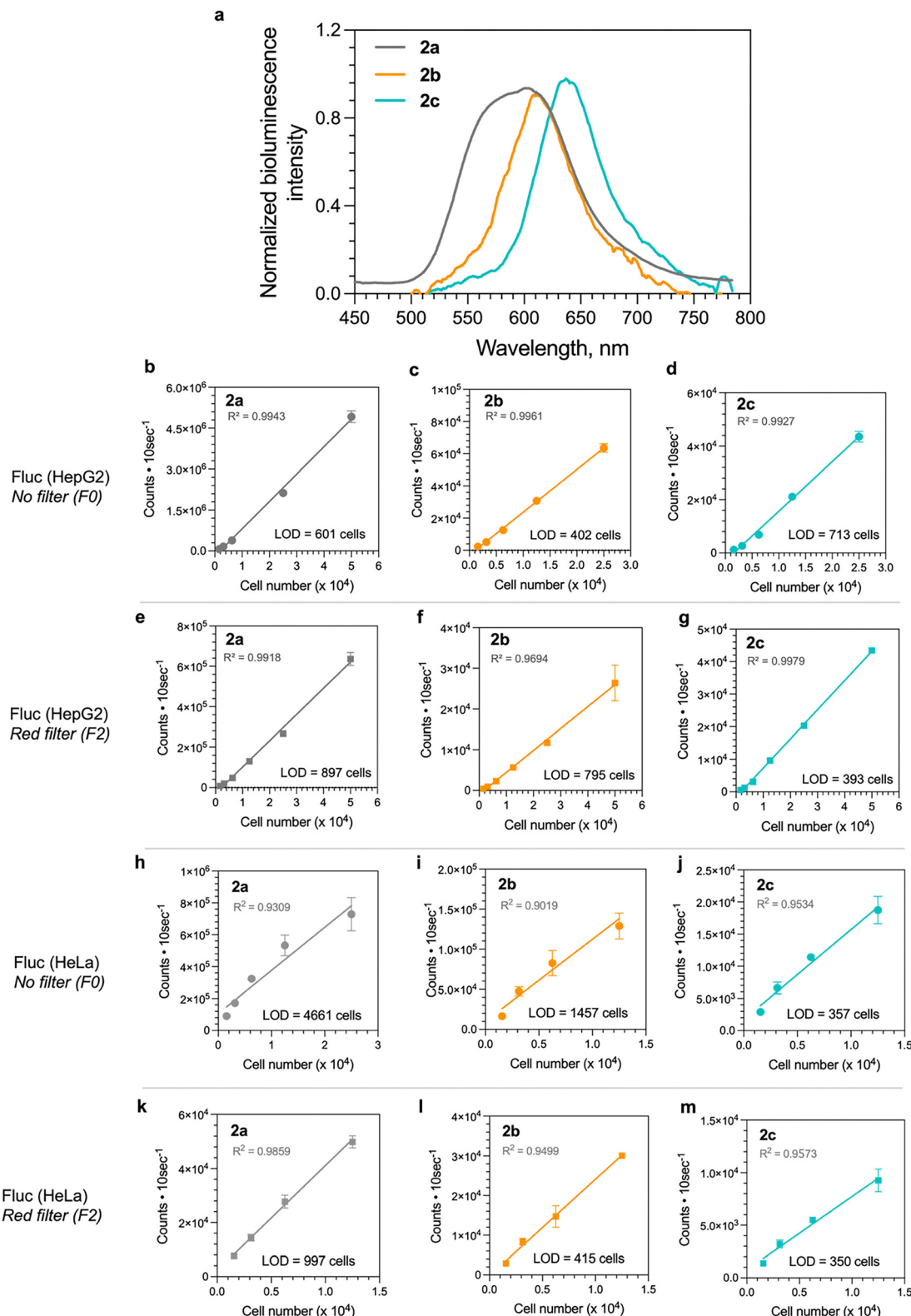
© 2026 The Author(s). Published by the Royal Society of Chemistry

RSC Chem. Biol., 2026, **7**, 67–80 | 75

Fig. 7 BL characteristics and applications of D-LH$_2$ analogues (**2a–2c**) in live cells. (a) The BL spectra of Fluc and D-LH$_2$ analogues (**2a–2c**) in stable reporter HepG2 cell lines harboring the fluc gene. The spectra were measured in live cells in 25 mM HEPES-NaOH pH 7.0 containing DMEM culture medium at 37 °C. The use of D-LH$_2$ analogues (**2a–2c**) in living HepG2 cells. D-LH$_2$ analogues were tested for their detection sensitivities by varying the number of HepG2 reporter cells using different BL filters including F0 (no filter) and F2 (red filter, >620 nm long-pass filter). (b–d) Linearity ranges of HepG2 cell number detection using **2a**, **2b**, and **2c** with the F0 filter. (e–g) Linearity ranges of HepG2 cell number detection using **2a**, **2b**, and **2c** with the F2 filter. The detection sensitivities of HeLa cells expressing fluc gene by transient transfection were tested with D-LH$_2$ analogues using different BL filters including F0 (no filter) and F2 (red filter, >620 nm long-pass filter). (h–j) Linearity ranges of HeLa cell number detection using **2a**, **2b**, and **2c** with the F0 (no filter). (k–m) Linearity ranges of HeLa cell number detection using **2a**, **2b**, and **2c** with the F2 filter.

stably expressing a Fluc reporter (details are given in SI, Section S1.6). The BL spectra in intact cells were captured using a highly sensitive CCD spectrophotometer with 2 min exposure time. The spectra in Fig. 7a and Fig. S21 showed a broad spectrum of **2a**-Fluc in live cells with a peak at 604 nm, which differed from those of the purified Fluc reactions (Fig. 4f). However, the spectra of **2b** and **2c** in living cells were identical to those of the purified Fluc reactions (refer to Fig. 7a and 4f) with red-shifted wavelengths at 609 and 638 nm, respectively. HepG2 and HeLa cell lines were chosen for further investigation because they are among the most commonly used cell lines in biomedical research (41 200 and 46 000 publications in 2023, respectively, searched by Google Scholar, Fig. S20).

We further investigated the sensitivity of reporter HepG2 and HeLa cell line detection when **2a–2c** were used as substrates. The number of HepG2 and HeLa cell lines was varied by 2-fold dilution and the cells were seeded in a 96-well plate. 100 μM (final concentration) of **2a–2c** in culture medium was then added to the cells and incubated for 30 min. The BL signals (photon counts) after a 30 min incubation period were measured with different filters to increase the selectivity for the BL wavelength—especially towards red-shifted light. In this work, we used optical filters including F0 (no filter) and F2 (red filter, >620 nm long-pass filter) to enhance the BL signals at specific wavelength regions to reduce background signals. The detection of live HepG2 and HeLa cell lines using an F0 filter (no filter) in Fig. 7b–m showed a good linearity ($R^2 > 0.99$) with all compounds (**2a–2c**). The sensitivity for detection in live Fluc-expressing HepG2 cells using **2b** was better than those of **2a** and **2c**, with an LOD of approximately 402 cells in the assay, using the F0 filter (no filter). The results in Fig. 7e–g showed linearity ranges for detection by **2a–2b** measured using the F2 filter, which collected light signals >620 nm. **2c** showed a prominent ability of red emitted signals for live cell detection in red BL regions, displaying high sensitivity when measured in HepG2 cells with a red filter, which required only 393 cells. In contrast, LODs for the similar systems with **2a** and **2b** are 897 and 795 cells, respectively (Table 3).

Interestingly, the sensitivity for detection in live Fluc-expressing HeLa cells treated with **2c** gave an LOD of approximately 357 cells which had higher sensitivity than those of **2b** and **2a** about 4.1 and 13.0-fold, respectively, using the F0 filter (no filter) (Fig. 7h–j and Table 3). Detection using the F2 filter for HeLa reporter cells also showed the LODs with **2c**, **2b**, and **2a** as 350, 415, and 997 cells, respectively (Fig. 7k–m and Table 3). The HeLa cells with **2c** gave higher sensitivity than that of **2a** about 2.8-fold using the F2 filter.

We further tested the usage of D-LH$_2$ analogues (**2a–2c**) with SLR and Pmluc-N230S expressing HepG2 and HeLa cells. Results in Fig. S22 and S23 and Table 3 indicate that most of the red-shifted D-LH$_2$ (**2b** and **2c**) provided higher sensitivity with lower LOD values than that of **2a**, except for Pmluc-N230S-expressing HepG2 and HeLa cells treated with **2c**.

The results suggested that methyl-substituted luciferins (**2b** and **2c**) can permeate through the cell membrane of live cells and serve as substrates for Fluc inside the cytosol well. The high

Table 3 Detection sensitivities of luciferase-expressing cells treated with D-LH$_2$ analogues using different optical filters

Reporter cell	Filter	Limit of detection (LOD), cells		
		2a	**2b**	**2c**
Fluc (HepG2)	F0	601	402	713
SLR (HepG2)		802	643	500
Pmluc-N230S (HepG2)		2010	752	ND[a]
Fluc (HepG2)	F2	897	795	393
SLR (HepG2)		1071	783	613
Pmluc-N230S (HepG2)		1880	247	ND[a]
Fluc (HeLa)	F0	4661	1457	357
SLR (HeLa)		1352	973	1437
Pmluc-N230S (HeLa)		1428	630	ND[a]
Fluc (HeLa)	F2	997	415	350
SLR (HeLa)		1268	826	707
Pmluc-N230S (HeLa)		1185	812	ND[a]

[a] ND denotes "not determined" because **2c** gave weak BL signals.

light intensity of **2b** in this red BL region also demonstrated its ability to serve as a new substrate (in replacement of **2a**) for luciferases. **2c** also showed high BL signals at longer red-shifted wavelengths which was suitable for detecting luciferase-expressing cells in low numbers because it provides high sensitivity for red light emission.

The reporter HepG2 cell line expressing Fluc, SLR, and Pmluc-N230S was also real-time monitored after adding 100 μM (final concentration) of D-LH$_2$ analogues (**2a–2c**) in Fig. 8a–i. The BL characteristics of all D-LH$_2$ analogues in live cells were measured for 3 days. The results showed that the light intensity of **2b** in stable Fluc-expressing reporter cells was slightly higher than that of **2a** for 24 h when measured using both F0 and F2 filters and then gradually decreased over time after 30 h. **2c** showed greater red BL signals (highest F2/F0 ratio) than other compounds but gave lower BL intensity than **2a** and **2b** when using the F0 filter or no filter was used (Fig. 8a–c). The highest BL signals of **2a–2c** could be achieved at 44, 35, and 6 h, respectively. The data indicate that the highest signals of **2c** and **2b** BL could be obtained at 7.3 and 1.2-fold faster rates than that of **2a**, respectively. This may be due to the ability of **2b** and **2c** to penetrate the cells faster than **2a**.

The transient SLR-expressing HepG2 cells with **2b** showed faster light generation kinetics, which gradually decreased after 10 h. The real-time BL signal patterns of **2a** and **2c** were also similar to that of **2b**, with **2c** exhibiting the highest F2/F0 ratio (red BL characteristics) than those of **2a** and **2b** (Fig. 8d–f). The transient Pmluc-N230S-expressing HepG2 cells showed similar kinetic patterns with all compounds **2a–2c** (Fig. 8g–i). The cells with **2b** and **2c** appeared to prolong the BL signals after 40 h better than that of **2a**.

Moreover, when the HeLa cell lines transiently expressing Fluc, SLR, and Pmluc-N230S were treated with 100 μM (as a final concentration) of D-LH$_2$ analogues (**2a–2c**), their real-time monitored kinetic characteristics were different from those of HepG2 cells (Fig. S24). The highest BL signals could be achieved approximately at 510 h. After a maximum peak at
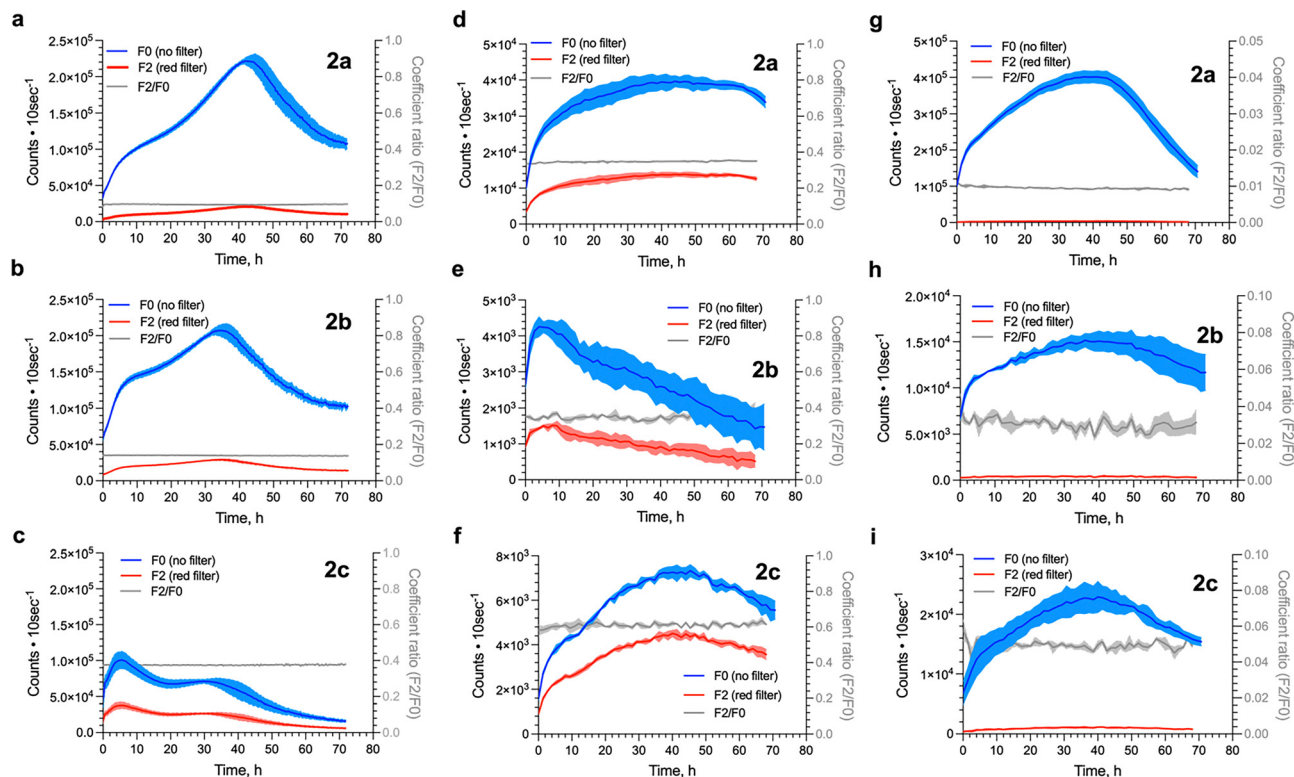
Fig. 8 Real-time monitoring of BL signals of HepG2 cell lines with luciferase reporters and D-LH$_2$ analogues (**2a–2c**). (a–c) BL real-time monitoring signals of stably Fluc-expressing HepG2 cells with natural D-LH$_2$ (**2a**), 5′-MeLH$_2$ (**2b**), and 5′,7′-DiMeLH$_2$ (**2c**), respectively. (d–f) BL real-time monitoring signals of transient transfection of SLR reporter in HepG2 cells with natural D-LH$_2$ (**2a**), 5′-MeLH$_2$ (**2b**), and 5′,7′-DiMeLH$_2$ (**2c**), respectively. (g–i) BL real-time monitoring signals of transient transfection of Pmluc-N230S reporter in HepG2 cells with natural D-LH$_2$ (**2a**), 5′-MeLH$_2$ (**2b**), and 5′,7′-DiMeLH$_2$ (**2c**), respectively.

5 h, the BL signal of the **2a** compound (a native D-LH$_2$) with Fluc-expressing HeLa cells gradually decreased. BL signals of **2b** and **2c** could be prolonged much better, up to 13 h before decreasing (Fig. S24b and c). Similarly, the kinetics patterns in SLR-expressing HeLa cells (Fig. S23d–f) showed more prolonged BL signals (up to 18 h) with **2c** than those of **2a** and **2b** compounds (up to 10 h) before signal decreasing. The Pmluc-N230S-expressing HeLa cells exhibited low BL signals with all **2a–2c** compounds, particularly with the **2c** compound (Fig. S23g and h). Kinetics of these BL signals indicate the ability of these D-LH$_2$ analogues (**2a–2c**) to penetrate the cell membrane and maintain their activities inside the cells.

All results suggest that D-LH$_2$ analogues with a methyl substituent at the benzothiazole ring, including **2c** and **2b**, can penetrate the cells faster than natural D-LH$_2$ (**2a**). Therefore, **2b** and **2c** showed great potential to be used as substrates for cell-based assays and real-time monitoring experiments.

Conclusions

Here, we developed a new setup for cost-effective one-pot green synthesis of six D-LH$_2$ analogues using mild chemical reagents. We discovered that by establishing a continuous feeding of D-cys (2 eq.) into an anaerobic one-pot reaction containing anaerobic **1a** (1 eq.), the substrate instability (**1a** derivatives and D-Cys) and yield of D-LH$_2$ analogues could be significantly improved. The process could improve the production yield by 63-fold compared to the previously reported chemical condensation method.[17] The synthesis method here could synthesize two new D-LH$_2$ analogues including 5′,7′-DiMeOLH$_2$ (**2d**) and 7′-MeNpLH$_2$ (**2f**). Substituents such as methyl, methoxy, and naphthol groups at the luciferin′s benzothiazole ring (**2b–2f**) generated longer red-shifted BL wavelength than that of the natural D-LH$_2$ (**2a**) by up to 88 nm when reacting with five types of beetle luciferases. The longest red-shifted BL could be obtained from the **2d**-SLR orthogonal pair reaction with a maximum BL at 663 nm. However, the reactions of luciferases with **2d** and **2f** gave low signals; this requires enzyme engineering to improve the BL signals of **2d** and **2f** in the future.

We demonstrated the use of D-LH$_2$ analogues (**2a–2f**) in mammalian cell lines. The crude lysate assays exhibited good light intensity in the reactions of **2b** and **2c** in HepG2, HEK293T, HeLa, and RAW264.7 cells, especially **2b** provided greater detection sensitivity of the Fluc enzyme in crude lysates than **2a** by about 11.2-fold; this is beneficial for bio-reporter and cell-based assay applications. Real-time BL measurements in live cells showed that **2b** and **2c** provide greater BL red-shifted signals than **2a**. Altogether, our results indicate that a small methyl group substituent in the luciferin′s benzothiazole

ring does not disrupt the activity of wild-type beetle luciferases but enhances light intensity, red-shifted BL, and provided greater light stability—features that are highly advantageous for *in vitro*, *ex vivo*, and *in vivo* BL detection applications in the future.

Author contributions

P. W. and P. C. designed experiments; P. W., I. K., P. K., C. K., and D. S. performed experiments. I. K., W. J. and P. W. elucidated the structures of synthesized D-LH$_2$ analogues by QTOF-MS and NMR. P. W. and C. K. optimized the conditions of bioluminescence assays. P. W. characterized the synthesized D-LH$_2$ analogues. N. L. and A. P. performed molecular docking and MD simulations. P. W., I. K., P. K., W. J., C. K., D. S., A. P., N. L., S. V., R. T., S. M., J. S., Y. N. and P. C. performed the data analysis. P. C., R. T., S. M., J. S., R. N., K. N., Y. N., and Y. O. provided advice. P. W. and P. C. wrote the manuscript with suggestions and comments from all authors.

Conflicts of interest

A patent application related to synthesis of red-shifted luciferin analogues has been submitted to the Department of Intellectual Property, Thailand (TH 2301002330).

Data availability

The authors declare that all data supporting the findings of this study are available within the paper and its supplementary information (SI). Supplementary information: experimental procedures, tables and figures showing D-LH$_2$ analogue synthesis, yield optimization, structural elucidation and bioluminescence characterization, and molecular docking, and applications of D-LH$_2$ analogues in crude lysates and live mammalian cell lines. See DOI: **https://doi.org/10.1039/d5cb00287g**.

Acknowledgements

Notes and references

1 A. C. Love and J. A. Prescher, *Cell Chem. Biol.*, 2020, **27**, 904–920.

2 N. Thorne, J. Inglese and D. S. Auld, *Chem. Biol.*, 2010, **17**, 646–657.

3 Y. Ando, K. Niwa, N. Yamada, T. Enomoto, T. Irie, H. Kubota, Y. Ohmiya and H. Akiyama, *Nat. Photonics*, 2008, **2**, 44–47.

4 M. S. Evans, J. P. Chaurette, S. T. Adams, G. R. Reddy, M. A. Paley, N. Aronin, J. A. Prescher and S. C. Miller, *Nat. Methods*, 2014, **11**, 393–395.

5 A. Yevtodiyenko, A. Bazhin, P. Khodakivskyi, A. Godinat, G. Budin, T. Maric, G. Pietramaggiori, S. S. Scherer, M. Kunchulia, G. Eppeldauer, S. V. Polyakov, K. P. Francis, J. N. Bryan and E. A. Goun, *Nat. Commun.*, 2021, **12**, 2680.

6 C. L. Stowe, T. A. Burley, H. Allan, M. Vinci, G. Kramer-Marek, D. M. Ciobota, G. N. Parkinson, T. L. Southworth, G. Agliardi, A. Hotblack, M. F. Lythgoe, B. R. Branchini, T. L. Kalber, J. C. Anderson and M. A. Pule, *eLife*, 2019, **8**, e45801.

7 S. Liu, Y. Su, M. Z. Lin and J. A. Ronald, *ACS Chem. Biol.*, 2021, **16**, 2707–2718.

8 A. J. Syed and J. C. Anderson, *Chem. Soc. Rev.*, 2021, **50**, 5668–5705.

9 M. Kiyama, S. Iwano, S. Otsuka, S. W. Lu, R. Obata, A. Miyawaki, T. Hirano and S. A. Maki, *Tetrahedron*, 2018, **74**, 652–660.

10 Z. Yao, D. R. Caldwell, A. C. Love, B. Kolbaba-Kartchner, J. H. Mills, M. J. Schnermann and J. A. Prescher, *Chem. Sci.*, 2021, **12**, 11684–11691.

11 S. Iwano, M. Sugiyama, H. Hama, A. Watakabe, N. Hasegawa, T. Kuchimaru, K. Z. Tanaka, M. Takahashi, Y. Ishida, J. Hata, S. Shimozono, K. Namiki, T. Fukano, M. Kiyama, H. Okano, S. Kizaka-Kondoh, T. J. McHugh, T. Yamamori, H. Hioki, S. Maki and A. Miyawaki, *Science*, 2018, **359**, 935–939.

12 R. Ono, K. Osawa, Y. Takahashi, Y. Noguchi, N. Kitada, R. Saito-Moriya, T. Hirano, S. A. Maki, K. Shibata, H. Akiyama, K.-I. Kanno, H. Itabashi and M. Hiyama, *J. Photochem. Photobiol., A*, 2023, **434**, 114270.

13 Z. M. Kaskova, A. S. Tsarkova and I. V. Yampolsky, *Chem. Soc. Rev.*, 2016, **45**, 6048–6077.

14 D. C. McCutcheon, W. B. Porterfield and J. A. Prescher, *Org. Biomol. Chem.*, 2015, **13**, 2117–2121.

15 S. J. Williams and J. A. Prescher, *Acc. Chem. Res.*, 2019, **52**, 3039–3050.

16 P. Watthaisong, P. Kamutira, C. Kesornpun, V. Pongsupasa, J. Phonbuppha, R. Tinikul, S. Maenpuen, T. Wongnate,

© 2026 The Author(s). Published by the Royal Society of Chemistry

RSC Chem. Biol., 2026, **7**, 67–80 | 79

R. Nishihara, Y. Ohmiya and P. Chaiyen, *Angew. Chem., Int. Ed.*, 2022, **61**, e202116908.

17 S. Kanie, T. Nishikawa, M. Ojika and Y. Oba, *Sci. Rep.*, 2016, **6**, 24794.

18 P. Watthaisong, P. Pongpamorn, P. Pimviriyakul, S. Maenpuen, Y. Ohmiya and P. Chaiyen, *Angew. Chem., Int. Ed.*, 2019, **58**, 13254–13258.

19 P. Anastas and N. Eghbali, *Chem. Soc. Rev.*, 2010, **39**, 301–312.

20 E. H. White, E. Rapaport, H. H. Seliger and T. A. Hopkins, *Bioorg. Chem.*, 1971, **1**, 92–122.

21 S. J. Williams, C. S. Hwang and J. A. Prescher, *Biochemistry*, 2021, **60**, 563–572.

22 T. Noguchi, M. Ikeda, Y. Ohmiya and Y. Nakajima, *PLoS One*, 2012, **7**, e37093.

23 Y. Nakajima, T. Yamazaki, S. Nishii, T. Noguchi, H. Hoshino, K. Niwa, V. R. Viviani and Y. Ohmiya, *PLoS One*, 2010, **5**, e10011.

24 O. Yoshihiro, H. Takashi and O. Mamoru, *FEBS Lett.*, 1996, **384**, 83–86.

25 Y. Ohmiya, N. Ohba, H. Toh and F. I. Tsuji, *Photochem. Photobiol.*, 1995, **62**, 309–313.

26 V. Viviani, A. Uchida, N. Suenaga, M. Ryufuku and Y. Ohmiya, *Biochem. Biophys. Res. Commun.*, 2001, **280**, 1286–1291.

27 M. Kato, K. Tsuchihashi, S. Kanie, Y. Oba and T. Nishikawa, *Sci. Rep.*, 2024, **14**, 30461.

28 Y.-M. Zhang, J. Zhang and S. X.-A. Zhang, *Dyes Pigm.*, 2017, **138**, 1–6.

29 K. P. Asare, M. Zniber, M. Zouheir, L. Wang, X. Wang and T.-P. Huynh, *MRS Commun.*, 2022, **12**, 90–94.

30 S. M. Marques and J. C. G. Esteves da Silva, *IUBMB Life*, 2009, **61**, 6–17.

31 J. Phonbuppha, R. Tinikul, Y. Ohmiya and P. Chaiyen, *J. Biol. Chem.*, 2023, **299**, 104639.

32 G. Morciano, A. C. Sarti, S. Marchi, S. Missiroli, S. Falzoni, L. Raffaghello, V. Pistoia, C. Giorgi, F. Di Virgilio and P. Pinton, *Nat. Protoc.*, 2017, **12**, 1542–1562.

33 H. W. Lee, Y. H. Jeon, M.-H. Hwang, J.-E. Kim, T.-I. Park, J.-H. Ha, S.-W. Lee, B.-C. Ahn and J. Lee, *Mol. Imaging Biol.*, 2013, **15**, 703–712.

34 Y. J. Choi, S.-G. Oh, T. D. Singh, J.-H. Ha, D. W. Kim, S. W. Lee, S. Y. Jeong, B.-C. Ahn, J. Lee and Y. H. Jeon, *Neoplasia*, 2016, **18**, 133–141.